Geant4 simulation of the neutron backscattering technique in farm soil for landmine detection

Daniel Alejandro Andrade Rodríguez

Universidad Nacional de Colombia
Facultad de Ciencias
Departamento de Física
Grupo de física nuclear - GFNUN

Advisor Prof. Fernando Cristancho

December 5, 2014

Contents

List of Figures

Chapter 1

Introduction

In the field of land mine detection, many techniques have been studied, from electromagnetic inductions techniques which is based in induced electric currents in the components of the mine, to acoustic techniques which are based in the reflection of sound or seismic waves off mines, any of them with strengths and limitations [1]. Among the conventional techniques, nuclear techniques have shown advantages due to the fact that landmines contains no metal parts but mainly organic materials, which escapes detection using conventional methods. One of the techniques that are being studied at the Universidad Nacional de Colombia by the Nuclear Physic Group (GFNUN) [2] [3] and in different countries [4] is the Neutron Backscattering Technique (NBT) which is based in the fact that a buried object target have high content of hydrogen and therefore if it is in a media with different hydrogen content and if it is exposed to a fast neutron source, the number of backscattered thermal neutrons produced by the moderation process of the landmine will give us a signal from which we can infer the presence and location of the landmine.

In the case of nuclear techniques like NBT is necessary to understand the advantages, the disadvantages and the limit of applicability in the case of it in the Colombian case. One of the most important issues is the presence of moisture in the soil, and this is one of the topics treated in the present work. The presence of an extra amount of water content in the soil implies an extra amount of hydrogen that will generate a background in the distribution of the backscattered neutrons. If the hydrogen content of the soil is similar to the content present in the landmine this will be no detected. In the present work the NBT technique is studied using simulation via the Geant4 toolkit also in different types of soil (sand and farm soil) taking into account the moisture content in both cases and taking into account the soil composition.

The present work presents a basic introduction of the neutron matter interaction in Chapter 2 reviewing basic aspects as the ways of a neutron could lose energy when it interacts, as well how the neutrons could reach thermal energies, which is the mainly idea of the neutron backscattering technique. In Chapter 3 a brief review of the technique is done, some details of the implementation using the Geant4 toolkit are presented. Finally in Chapter 4 a review of the results is done, considering the aspects implemented, as the moisture content and the soil composition for different cases.

Chapter 2

The interaction of neutrons with matter

The neutron lacks an electric charge, so it is not subject to Coulomb interactions with the electrons and nuclei in matter. Instead, its principal means of interaction is through the strong force with the nuclei. These kind of reactions are much rarer because of the short range of this force. Neutrons must approach within 10^{-3} cm of the nucleus before any reaction can happen, and since normal matter is mainly empty space the neutron is observed to be a very penetrating particle [5].
When the neutron does interact, it may undergo a variety of nuclear processes depending of its energy:

- Elastic scattering from nuclei. This is the principal mechanism of energy loss for neutrons in the MeV region.
- Inelastic scattering. In this reaction is left in an exited state which may later decay by γ-ray or some other form of radiative emission. To get inelastic reaction, the neutron must have sufficient energy to excite the nucleus i.e in the order of 1 MeV or more. Below this energy elastic scattering may occur.
- Radiative neutron capture. In general the cross section for neutron capture goes approximately as $1/v$ where v is the velocity of the neutron. Absorption its most likely at low energies.
- Other nuclear reactions, such as (n,p), (n,d), (n,α), (n,t), etc. in which the neutron is captured and charged particles are emitted. This generally occurs in the eV to keV region.
- Fission. This kind of reaction is most likely at thermal energies.
- High energy hadron shower production. This occurs only for high energy neutrons ($E > 100$ MeV).

Neutron are classified according to its kinetic energy, this because its strong dependence on interactions:

- High energy neutrons: those with energies above 100 MeV.
- Fast neutrons: those between few ten's of MeV and a few hundred of keV.
- Epithermal: between ≈ 100 keV and ≈ 0.1 eV.
- Thermal: at low energies comparable with the thermal agitation energy at room temperature $T = 21°\text{C} \rightarrow E \approx kT \approx 0.025$ eV.
- Cold: meV to μeV.

The total probability for a neutron to interact with matter is given by the sum of the individual cross sections for each nuclear processes depending on its energy:

$$\sigma_{tot} = \sigma_{elastic} + \sigma_{inelastic} + \sigma_{capture} + \dots \tag{2.1}$$

Multiplying (2.1) by the density of atoms we can obtain the mean free path length:

$$\frac{1}{\lambda} = N\sigma_{tot} = \frac{N_a \rho}{A}\sigma_{tot} \tag{2.2}$$

so, the mean free path is

$$\lambda = \frac{A}{N_a \rho \sigma_{tot}} \tag{2.3}$$

Where ρ and A are the mass density and the atomic weight of the target respectively and N_a is the Avogadro's number.

Like photons, a beam of N neutrons passing through matter will be exponentially attenuated:

$$N = N_0 \exp(-x/\lambda), \tag{2.4}$$

where x is the thickness of the material and N_0 is the number of incident neutrons. It is usual to call $\mu = \frac{1}{\lambda}$, the *attenuation coefficient* and the ratio $\frac{N}{N_0}$ the *survival probability*, i.e, the probability that a neutron goes through the material without any interaction. Expression (2.4) is useful only for a collimated beam of neutrons [5].

2.1 Moderation process: Slowing down the neutrons

The slowing down of a fast neutron is know as moderation and is an important process in nuclear physics and engineering. A fast neutron entering into matter will scatter back and forth on the nuclei, both elastically and inelastically, losing energy until it gets thermal equilibrium with the surrounding atoms. At this point it will defuse through matter until it is finally captured by a nucleus or enters into other type of nuclear reaction e.g fission.
Elastic scattering is the principal mechanism of energy loss for fast neutrons. Let consider a single collision in the lab frame of reference between a neutron with velocity v_0 and a nucleus at rest with a mass M, working in units of a neutron mass i.e $m_n = 1$, so the mass of the neutron is just the atomic mass number A.

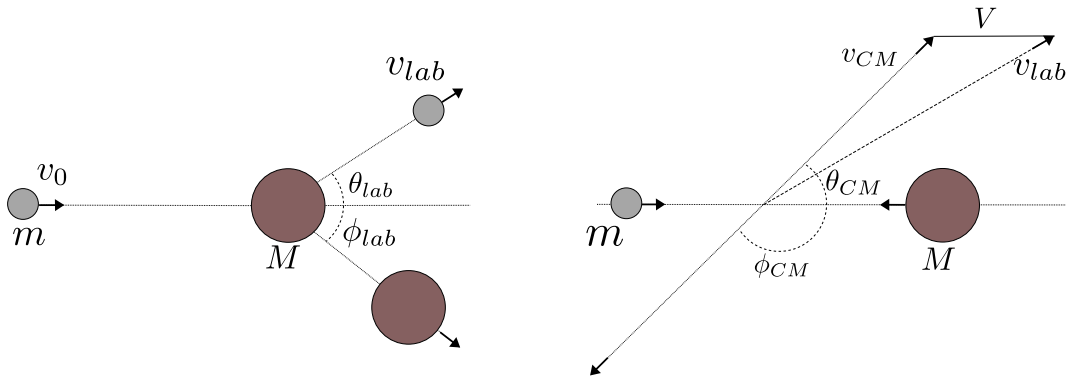

Figure 2.1: Elastic scattering in the laboratory system (left) and the center mass system (right). A neutron (mass m) with initial velocity v_0 is scattered by a target nucleus M initially at rest.

Transforming to the center mass system (CM), the velocity of the neutron becomes:

$$v_{cm} = \frac{A}{A+1} v_0 \tag{2.5}$$

and the nucleus takes a velocity

$$V = \frac{1}{A+1} v_0 \tag{2.6}$$

After the collision, the neutron goes on a new direction but remains its speed in the CM system. Using the law of cosines, the velocity of the neutron in the lab system is:

$$(v_{lab})^2 = (v_{cm})^2 + V^2 - 2 v_{cm} V \cos(\pi - \theta_{cm}) \tag{2.7}$$

where θ_{cm} is the center mass scattering angle. Substituting (2.5) and (2.6) into (2.7), we obtain: Taking into account that the kinetic energy is $E = \frac{1}{2} m v^2$, we have

$$\frac{E}{E_0} = \left(\frac{1/2 m v_{lab}^2}{1/2 m v_0^2} \right)^2 = \frac{A^2 + 1 + 2A \cos\theta_{CM}}{(A+1)^2} \tag{2.8}$$

From (2.8) we see now that the energy of the scattered neutron is limited to the range:

$$\left(\frac{A-1}{A+1} \right)^2 E_0 < E < E_0 \tag{2.9}$$

If $A = 1$ (the target nucleus is Hydrogen) the energy of the scattered neutron will fall on the interval:

$$0 < E < E_0 \tag{2.10}$$

This last result implies that for a single collision the incoming neutron has certain probability of transferring almost all its energy, reaching low or thermal energies, if the target has low atomic mass. The process of reaching thermal energies by elastic collisions is know as *thermalization* [5].

To know how many collisions are needed, in average, for a neutron reach thermal energies, the logarithmic change in energy is considered:

$$u = \ln \frac{E_0}{E}, \tag{2.11}$$

where E_0 is the initial energy and E the final energy. This is know as the *lethargy change*. From (2.8) we can get:

$$u(\theta) = \ln \frac{(A+1)^2}{A^2 + 1 + 2A\cos(\theta_{cm})}, \tag{2.12}$$

then, integrating over all the space and dividing by 4π we get the average lethargy:

$$\xi = 1 + \frac{(A-1)^2}{2A} \ln \frac{A-1}{A+1} \tag{2.13}$$

which is energy independent. The average number of collisions to reduce the neutron energy from E_0 to E is calculated as:

$$\overline{n} = \frac{u}{\xi} = \frac{1}{\xi} \ln \frac{E_0}{E} \tag{2.14}$$

Target	**A**	$\overline{n}$
Hydrogen	1	17.5
Helium	4	41.1
Carbon	12	110.9
Oxygen	16	146.9
Uranium	238	2088.8

Table 2.1: Average number of collisions to reduce the neutron's energy from 1 MeV to 0.025 eV for different targets.

In the case of a hydrogen target $A = 1$ and replacing A in (2.13) we obtain $\xi = 1$. In the case of a neutron beam with initial energy of $E_0 = 1$ MeV and we want to slow it down to thermal energies ($E = 0.025$ eV), we obtain

$$\overline{n} = \ln \frac{1\,\mathrm{MeV}}{0.025\,\mathrm{eV}} = 17.5\,\mathrm{collisions} \tag{2.15}$$

The table 2.1 shows the value of $\overline{n}$ for different targets. The value of $\overline{n}$ decreases when the number of nucleons in target increases. The minimum value is obtained for hydrogen, this implies that neutron beam will require less collisions to reach thermal energies interacting in hydrogen rich material, i.e, the thermalization process is more efficient in this material, fact that will used in the develop of the NBT.

2.2 Neutron detection

Due to the neutron charge absence its detection process is based in the production of charged particles by nuclear reactions. The strong dependence of the cross section of this reaction on the neutron energy has led to the development of different kinds of detectors depending on the neutron energy region. In figure (2.2) we see the total cross section for three different targets used in the thermal neutron detection process. The reaction $^3\text{He}(n,p)^3\text{H}$ has the highest cross section in the thermal region [6] and is the one used in the implementation of the NBT simulation setup .

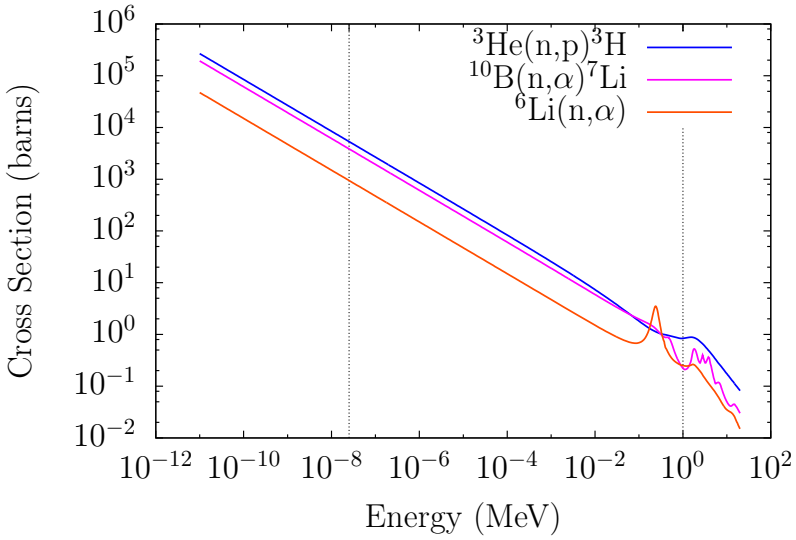

Figure 2.2: Total cross section for three different targets commonly used in the neutron detection (^{3}He, ^{6}Li and ^{1}0He) as a function of the incident neutron energy. The cross section for thermal neutrons ($E = 0.025\,\text{eV}$) is about 4 order of magnitude larger than the cross section for fast neutrons ($E = 1\,\text{MeV}$).

2.3 The ^{3}He proportional counter

In a ^{3}He + Ar based detector the reaction that take place is:

$$n + ^3\text{He} \rightarrow p + ^3\text{H} \qquad Q = 0.764\,\text{MeV} \tag{2.16}$$

A proton (p) and a triton atom (^{3}H) are produced in the reaction and they ionize the gas inside the detector. For thermal neutrons the cross section of this reaction is $\sigma = 5316\,\text{b}$ while for fast neutrons ($E \approx 1\,\text{MeV}$) is $\sigma = 0.83\,\text{b}$. This gives a high efficiency for thermal neutrons detection, and in the case of fast neutrons the probability of reactions is quite small.
The thermal neutrons energy is small compared with the Q of the reaction, and therefore the products will share the available energy [2]:

$$E_p + E_{^3\text{He}} = Q = 0.764\,\text{MeV} \tag{2.17}$$

Moment and energy conservation lead us to:

$$m_{^3\mathrm{He}} v_{^3\mathrm{He}} = m_p v_p \tag{2.18}$$
$$\sqrt{m_{^3\mathrm{He}} E_{^3\mathrm{He}}} = \sqrt{m_p E_p} \tag{2.19}$$

Solving equations (2.18) and (2.19) the products of the reaction will be produced in opposite directions with energies:

$$E_p = 0.573\,\mathrm{MeV} \tag{2.20}$$
$$E_{^3\mathrm{He}} = 0.191\,\mathrm{MeV} \tag{2.21}$$

2.4 The wall effect

The particles produced in the nuclear reaction inside the ^{3}He detector (p and ^{3}H) deposit their energy ionizing the gas in the detector. If the products are completely stopped inside the detector a peak at 0.764 MeV in the measured spectrum is expected. If the reaction occurs near to the wall of the detector it may happen that one of the products escape from the detector before depositing all its energy. This depends on the products range which also depends on the detectors characteristics as its pressure and density. If the range is comparable with the detector dimensions they have a higher probability to escape from the detector leaving only part of its energy. This phenomenon is know as *wall effect* and it will yield to a spectrum with a quasi-guassian peak at $E_p + E_{^3\mathrm{H}}$ with a long tail with a minimum energy at $E_{^3\mathrm{H}}$ [2].

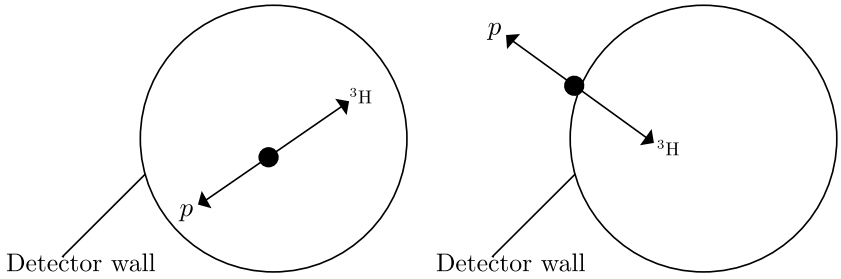

Figure 2.3: Product reaction inside the detector, if the reactions happens near to the detector wall, part of the energy could not be registered (right).

Chapter 3

The neutron backscattering technique

The principal characteristics of the neutron matter interaction have been described in the previous Chapters with the purpose of the neutron backscattering technique (NBT) and describe the process of landmine detecting. This chapter begins with the description of the NBT as well as the simulation setup. Then the description of the data analysis implemented to get an approximate value of where the landmine is buried as well the description of how the moisture content is implemented.

3.1 The simulation setup and data analysis

The NBT is based in the fact that the landmine has a high hydrogen content and the fast neutron emitted by a ^{252}Cf source can reach thermal energies more efficiently (less collisions) than in other targets as heavier nuclei. This characteristic of hydrogen was show in the section 2.1. Different approaches have been studied in the last years to implement this phenomena in a device capable of detecting landmines with high hydrogen content. In the present work the setup and data analysis proposed by Brooks [4] is follow. The simulation setup (figure 3.1) implemented for the NBT consist of eight cylindrical neutron detectors (^{3}He+Ar) placed in two arrays (labeled as A and B) and the fast neutron source (^{252}Cf) are placed above a soil box (sand or farm soil) in which the landmine to be detected is buried.

The detector arrays A and B separated a distance a with the neutron source move together along horizontal path parallel to the surface of the soil box (x coordinate). The fast neutrons emitted by the source separated a distance z from the surface of the soil, interacts with the soil and with the landmine buried at depth d mainly by elastic collisions. This because the cross section for elastic scattering is larger than the other cross sections for other processes. In elastic scattering the incoming fast neutron loses energy and if the landmine has high hydrogen content the number of thermal neutrons will increase as the detector system (source and detector arrays) approaches to it in the x coordinate. In a first aproximation the soil will be considered without any water content (dry soil) and then a moisture layer with depth w will be considered for study how the water content affects the number of counts registered. The main quantity to be measured in the NBT is the number of thermal neutrons that reach each detector in the arrays.

The procedure to detect the landmine consist first on measuring the numbers of counts in each detector of the arrays as a function of the x coordinate. The expected signal of this scan is show in figure 3.2.
The number of thermal neutrons increases in positions near to the landmine. The maximum of each distribution happens when the center of the object is midway between the source and the detector.

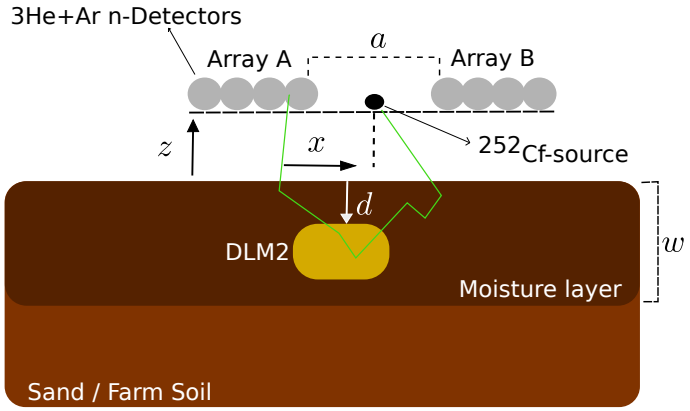

Figure 3.1: Simulation setup of the NBT for the detection of a landmine buried in two different kind of soils (sand and farm soil). The green line represent a random trajectory that a neutron emitted by the source could take. The neutron interacts with the soil, the landmine and finally is detected in one of the arrays.

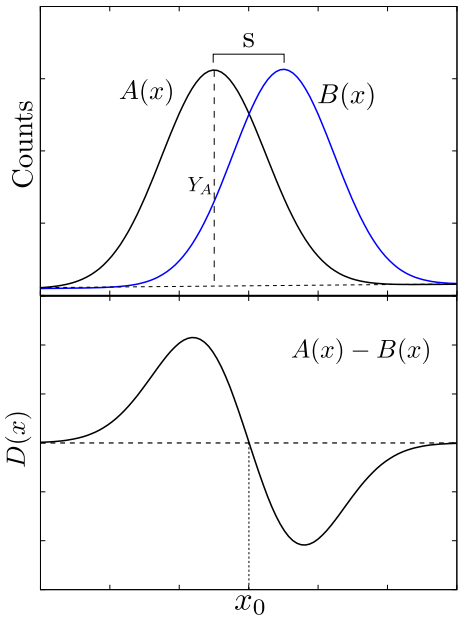

Figure 3.2: Expected response of a scan with the NBT setup for a landmine with high hydrogen content, located at x_0

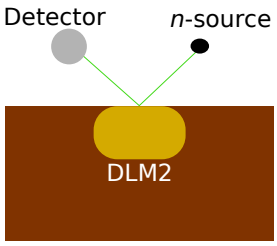

Figure 3.3: The maximum number of thermal backscattered neutrons is found in the x position where the center of the landmine is located, at midway between the source an the detector. The maximum is located in $x = x_0 - s$ for the a array and in $x = x_0 + s$ for the B array.

The probability of a fast neutron to be thermalized in the landmine and scattered in the direction of the detector is larger when these two distances are almost equal (fig. 3.3))
If the received signals ($A(x)$ and $B(x)$) which can be fitted as gaussian functions are subtracted we get the difference function $D(x) = A(x) - B(x)$ (Figure 3.2). The position x_0 where the function $D(x_0) = 0$ and goes from positive to negative values, indicates the position in which the landmine is buried. The signal of the arrays $A(x)$ and $B(x)$ as well as the counts difference will depend on parameters as:

- Stand-off distance (z).
- Arrays separation distance (a).
- Depth at which is buried the DLM2 (d)
- Amount of hydrogen and in general the composition of the landmine.
- Acquisition time per each position of the array.
- Moisture content in the soil.

In the present work the number of registered counts as a function of parameters as stand-off distance, depth at which the target is buried and moisture content is studied following [4] and all the analysis will be done with the data obtained of several runs of the simulation for each kind of soil. If a single detector is used in the technique, a strong dependence of the number of counts, respect to the parameter z is found, which implies that with small variations of it, produces larger counts differences that could be confused with the signal of a landmine. This is the reason why the use of two separated array neutrons detectors was proposed separated a distance a. If the signal of each detector are subtracted the dependence with the height of the system (arrays and neutron source) can be minimized [7].
In the experimental setup proposed by Brooks [4] (the HYDAD-D) two ^{3}He are used, in our case eight neutron detector are used, organized in two arrays: A and B with the purpose of increasing the number of neutrons detected.

3.2 Details of the implementation in Geant4

The dimensions and materials of the detectors are chosen in concordance with the ones present in GFNUN's laboratories.

3.2.1 Soil implementation

To have an accurate implementation of the NBT, aspects like the soil composition have to be taken into account as well as the landmine composition. For the soil two case will be studied, a review of the case in which sand is used soil and the case in which farm soil is used. For the implementation of dry sand (mainly SiO_2) with a density of $\rho = 1.4$ g/cm^3. In the case of farm soil the composition taken in (3.1) is used, with a density of $\rho = 0.6$ g/cm^3 for dry farm soil.

Element	Concentration [%]
$Si0_2$	61.3
Al_2O_3	13
Fe_2O_3	2.5
CaO	1.6
MgO	0.7
$Ti0_2$	0.6
Organic material	20.3

Table 3.1: Farm soil composition implemented in the simulation. The values are normalized to 100% due to the fact that the technique used for determining the components in this material (XFR) cannot determine heavy nuclei and organic material.

Soil material is a complex of diverse components, including plant and animal residues, living and dead soil microorganisms, and substances produced by these organisms and their decomposition in a forest for example leaf litter and woody material falls to the forest floor [8].
Very little is currently known about natural organic material. Researchers are unable to crystallize it, this is important because once you can crystallize the material, it can be isolated and studied with x-ray crystallography. This method is standard for determining unknown compounds. Organic matter has not been characterized either and no unique structure is known. The best way to characterize organic matter is by discovering chemical, physical, and thermodynamic properties of the matter. Analytical techniques are currently being discovered to allow this to happen. Table 3.2 shows the composition of organic matter implemented in the simulation.

Element	Concentration [%]
C	50
O	42
H	5
N	3

Table 3.2: Organic material composition implemented in the simulation. This is an approximation since no standard composition is known.

3.2.2 ^{252}Cf source and landmine implementation

The source used in the simulation is an spontaneous fission ^{252}Cf source. The fission can occur in many transuranium element with the release of neutrons along the fission fragments. These fragments as well can promptly decay emitting β and γ radiation. The half-life of this source is 256 years. The energy spectrum is continuous and exhibits a Maxwellian shape, as show in (3.4) [5].

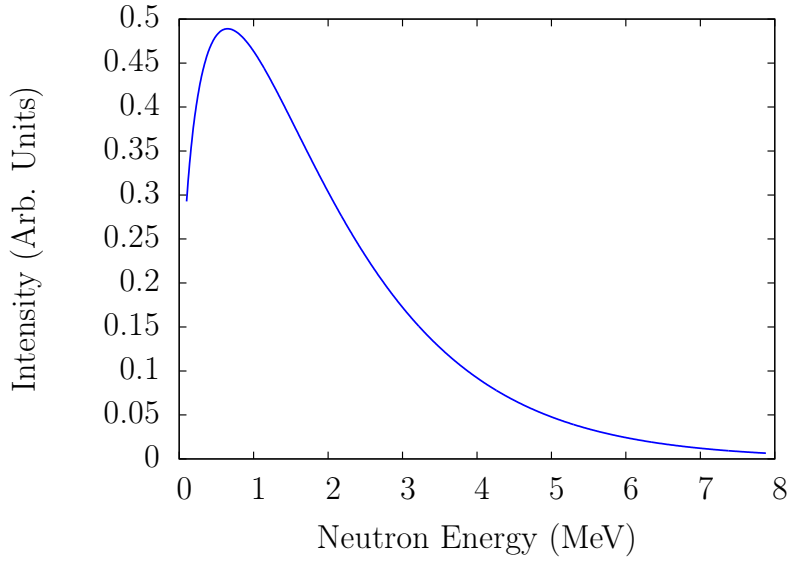

Figure 3.4: Implemented neutron energy spectrum from ^{252}Cf.

The distribution is described by:

$$\frac{dN}{dE} = \sqrt{E}\exp\left(\frac{-E}{T}\right) \tag{3.1}$$

where $T = 1.3\,\mathrm{MeV}$ for ^{252}Cf.
The dummy mine (DLM2) is provided by of the University of Cape Town. It consist of 100 g of TNT simulant inside an acrylic (polymethymethacrylate) container and is currently used in laboratory tests.

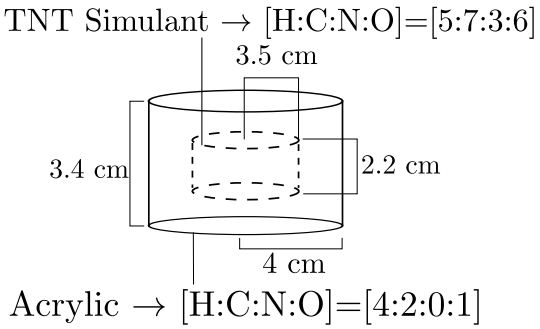

Figure 3.5: Elemental composition and picture of the dummy landmine used int the simulated setup of the NBT. The [H:C:N:O] brackets refers to the number of atoms of any kind that composes the molecule of the materials.

Chapter 4

Geant4 simulation of the neutron backscattering technique

Using the Geant4 toolkit, the NBT technique is implemented and the setup used is the one showed in 3.1, with the neutron detector, soil (sand and farm soil for different cases) and the ^{252}Cf source specifications. There are additional objects in the GFNUN laboratories that are also included in the simulation: the wood box container for the soil, a concrete column besides the box and a paraffin-lead shielding which contains the neutrons sources when it is not use [2] because this objects will also affect the measurements of the detectors.

4.1 NBT in dry soil

In a first approximation to the problem, the technique is simulated using sand as a soil, with the DLM2 placed at $d = 0$ cm (surface of the soil) and at $x = 0$ cm. A total of $N = 2.3 \times 10^6$ neutrons are emitted from the source for each x position of the detector system (array and source) in steps of $\Delta x = 5$ cm at each side from the center of the setup. This first scan is shown in figure 4.1.
The number of counts registered for each array as a function of the x coordinate($A(x)$ and $(B(x))$) is fitted as the following functions respectively:

$$A(x) = D_0 \exp\left(\frac{-(x - x_0 + s)^2}{\sigma^2}\right) + Y_B \tag{4.1}$$

$$B(x) = D_0 \exp\left(\frac{-(x - x_0 - s)^2}{\sigma^2}\right) + Y_B \tag{4.2}$$

where D_0 defines the amplitude of the fitted gaussians for each array and is related with the signal of the landmine, s is the displacement quantity between the two gussians, x_0 is the position of the landmine and σ is related with the half width of the gaussian at $0.6Y_0$ and σ will be also related with the geometry of the system and composition of the soil and landmine. The last term Y_B give us information about the soil composition and humidity content.
If we compare the signal obtained for the array A in figure 4.2 for both cases (sand and farm soil), we see that the amplitude registered in the case of sand is larger that in the case of farm soil for several reasons:

- The difference in the composition of the soil. In the case of sand there is only presence of SiO_2 meanwhile in farm soil several compounds are present in it (see table 3.1).

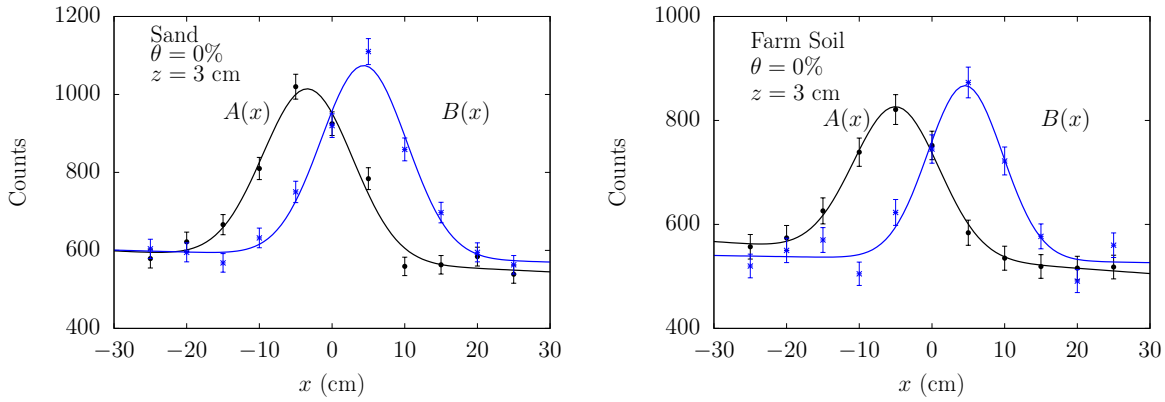

(a) Simulated NTB with sand.

(b) Simulated NTB with farm soil.

Figure 4.1: Geant4 simulation of the NBT for the DLM2 as a landmine placed at the surface of the soil (sand and) with depth $d = 0$ and position $x = 0$. The points are the simulation results and the lines are the fit for this data.

- The difference in density between both cases. Sand have a density of $\rho_s = 1.4$ g/cm^3 and farm soil has a density of $\rho_{fs} = 0.6$ g/cm^3. As it was shown in equation (2.2) if the density is large, the mean free path of the neutrons will be smaller and vice versa. This means that in the case of sand more interactions will happen before the neutrons can reach the landmine (some energy is lose in this process) but the major part of the thermalization process will occur in the landmine, due to the high hydrogen content as seen in table 2.1. This process is easier if the neutrons already lost some of its energy. For farm soil less interactions will occur before the neutron reach the landmine, (less energy is lost before the neutrons can reach the landmine) even with a small presence of hydrogen in farm soil.

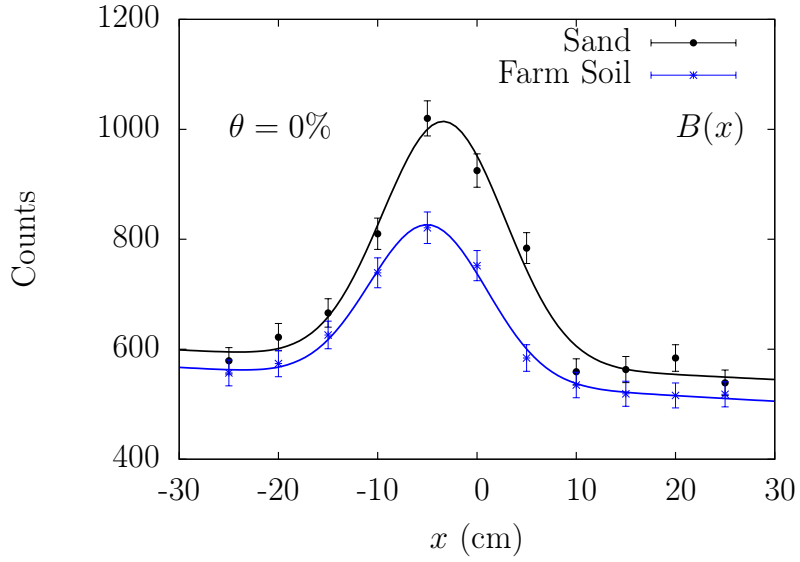

Figure 4.2: Comparison between the signal obtained in the array A for sand and farm soil.

Subtracting the two signals we obtain the difference function $D(x) = A(x) - B(x)$ showed in (4.3) and fitted as:

$$D(x) = \overline{D_0}\left\{\exp\left[\frac{-(x - x_0 + s)^2}{\overline{\sigma^2}}\right] - \exp\left[\frac{-(x - x_0 - s)^2}{\overline{\sigma^2}}\right]\right\}, \tag{4.3}$$

where $\overline{D_0}$ and $\overline{\sigma}$ are arithmetical averages of the parameters obtained in the fitting equations (4.1) and (4.2). $D(x)$ is constructed with the only purpose of localizing the mine (x_0) since no additional information is obtained.

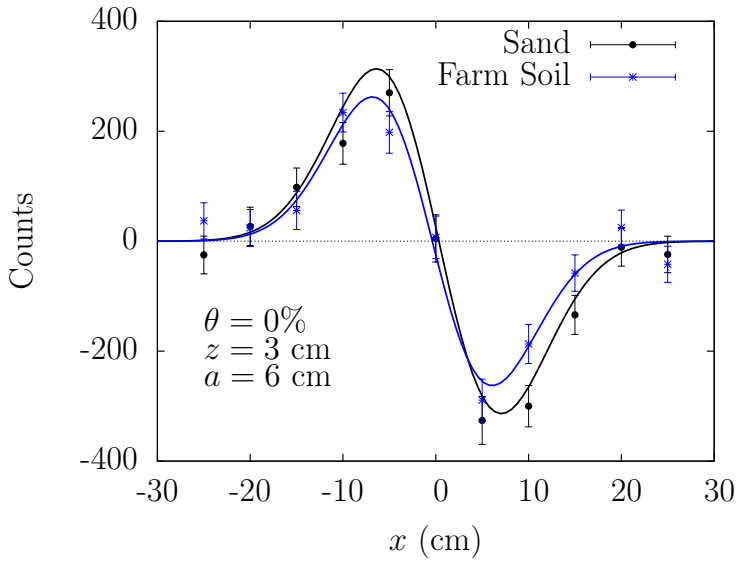

Figure 4.3: Difference signal $D(x) = A(x) - B(x)$ for sand and farm soil in the case in which the landmine is at the surface. The points are the simulation results and the line is the fit function for this data.

The difference function or signal is fitted as defined in equation (4.3), obtaining the following parameters:

	$\overline{D_0}$ (counts)	x_0 (cm)	$\overline{\sigma}$ (cm)	s (cm)
Sand	856(9)	0.3(3)	9.3(7)	2.6(6)
Farm soil	478(3)	-0.3(7)	8.7(6)	3.0(3)

Table 4.1: Parameters obtained defined in (4.3) for sand and farm soil for $d = 0$ cm and $x = 0$.

As we see the parameter x_0 gives us a good approximation on the x position of the landmine. The parameters of (4.1) will change as a function of the geometrical parameters previously mentioned (stand-off distance, depth at which the landmine is buried, etc).

In the experimental case a ^{252}Cf source with an activity of 1.15×10^6 n/s is used with an acquisition time of 2 seconds per x position in steps of $\Delta x = 5$ cm, this acquisition time is equivalent to the number of simulated neutron events per x position in the current implementation, this makes possible to do a directly comparison between the experimental results and the simulated ones, with the same

parameters. Figure (4.4) shows the signal for the array A in both cases, as we see the signal are almost the same, except some differences in the extreme points. This difference could be attributed to some external factors not included in the simulation.

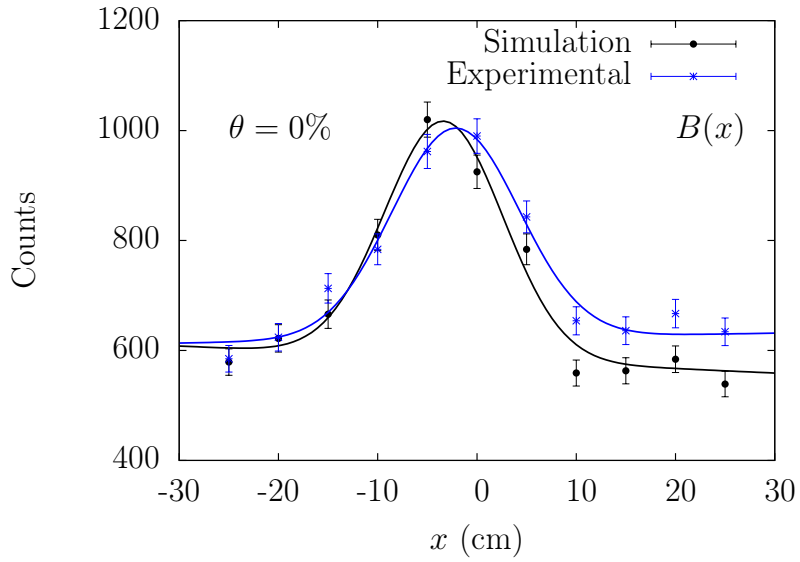

Figure 4.4: Comparison between the signal obtained from the array A in the case of the simulation and the experimental results obtained with the same parameters.

4.2 NBT with moisture in the soil

An important parameter to take into account for the NBT is the moisture content in the soil. The gravimetric content in soil [9] is defined as:

$$\theta_m = \frac{m_{H_2O}}{m_{soil}} \tag{4.4}$$

where m_{H_2O} is the mass of the water present in the soil and m_{soil} is the mass of the bulk of dry soil. Additional content of hydrogen in the soil, as in the case of farm soil, lead to an increase of the amplitude of the detected signals as well as the present background. Now a moisture layer (soil + water) is placed in the upper part of the soil box, simulating the process of percolation of water in granular media. The moisture layer is defined with a depth of $w = 18$ cm and as the previous case the DML2 is placed at $d = 0$ cm. Figure 4.2 shows different water contents for the moisture layer

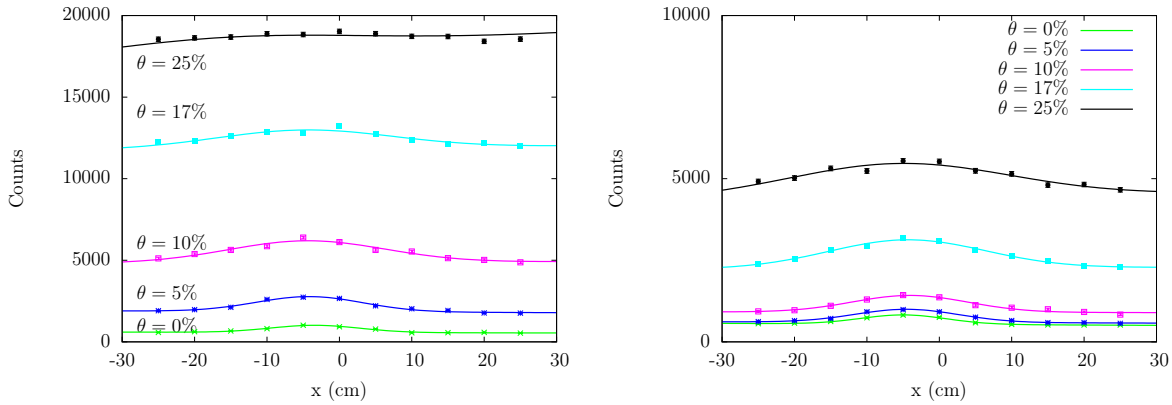

(a) Simulated signal for the array A in the case of sand. (b) Simulated signal for the array A in the case of farm soil.

Figure 4.5: Simulated $A(x)$ signal for different moisture values with the landmine at the surface $d = 0$ cm and the detectors arrays and source at $z = 3$ cm from the surface, for the case of sand and farm soil.

As we can see the amplitude and background of the signals detect is higher than the the case of dry soil due to the additional hydrogen content, this because an additional thermalization process is done in the soil. The increment of the amplitude as well as the detected background, produced by the landmine could be explained as prethermalization process in which the fast neutron that enters in the wet soil lose energy by elastic collisions with the hydrogen present in the water mixed in the soil, before they reach the landmine. In this case the neutrons that reach the landmine, do it with less energy that in the case of dry soil. As we see before, neutrons with less energy will require less collision to thermalize. This prethermalization process in the landmine produces the increment in the amplitude and the background of the detected signals [2].

The increment on the moisture content produce more thermal neutrons, this can be seen as an increment of the background as well as the increment of the amplitudes registered. With the proper calibration the number of counts far away from the object ($x > 20$ cm) or equivalent the parameter Y_B in (4.1) or (4.2) could give us a direct measurement of the moisture content in the soil.

For the moisture values defined, the difference function $D(x)$ is showed in figure 4.2. As expected the amplitudes of the functions $D(x)$ are increasing according together with increase of the moisture content. Although this process goes to a maximum value (in the case of sand $\theta_m \backsim 15\%$) and then decreases to a region in which no signal can be defined beyond that the background. The position of the landmine x_0 is well defined as the point in wich the functions $D(x)$ goes to zero counts and the values of the function goes from positive to negative.

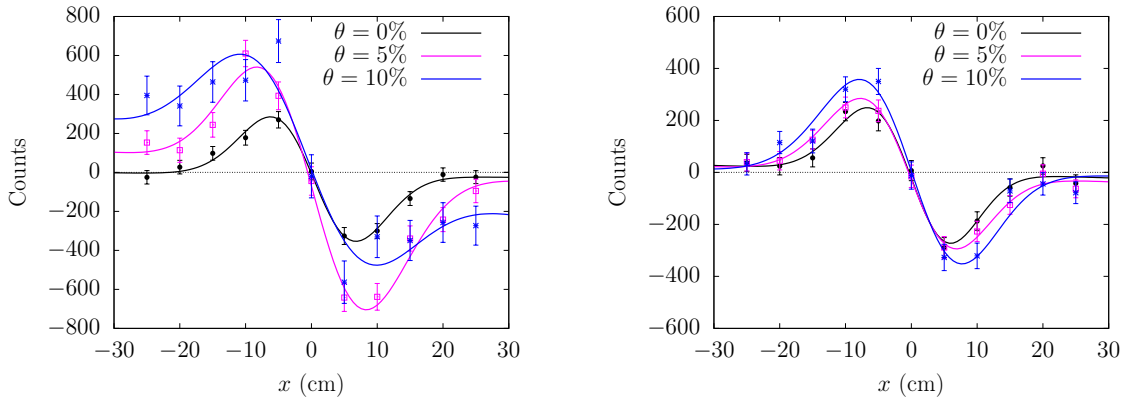

(a) Counts difference function $D(x)$ in the case of sand.

(b) Counts difference function $D(x)$ in the case of farm soil.

Figure 4.6: Counts difference function $D(x)$, for different moisture content. Some differences in the amplitude are observed due to the present of water in the soil

If the hydrogen content is elevated to a critical point the signal detected could disappear, this because the number of backscattered thermal neutrons that comes from the landmine thermalization process is equal to number of thermal neutrons backscattered by the wet soil and therefore no signal is obtained beyond the background. But as we see in figure 4.2, after the critical point of moisture an inversion of the signal is found, signal that preserves the characteristics before the critical point, and these signal can be used as well for determining the presence of the landmine.

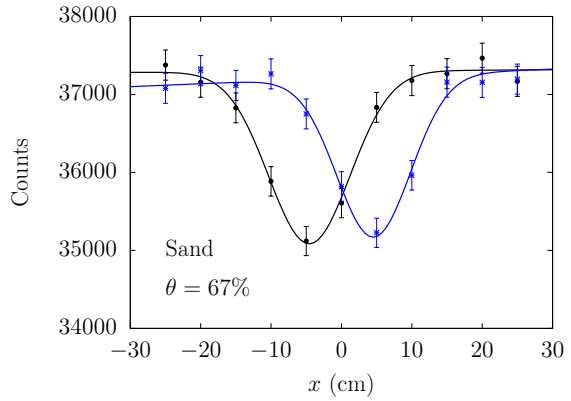

(a) Inversion of the signal obtained for both arrays with $\theta = 67\%$ in sand.

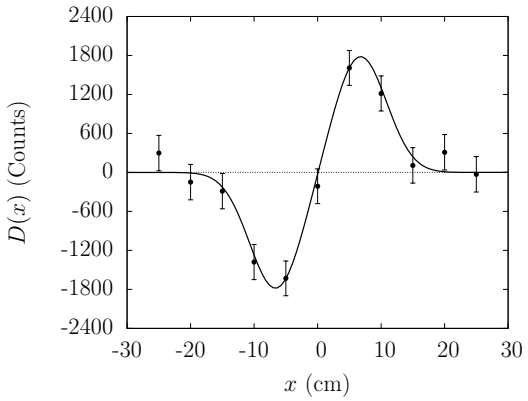

(b) Counts difference function $D(x)$ for $\theta = 67\%$ in sand.

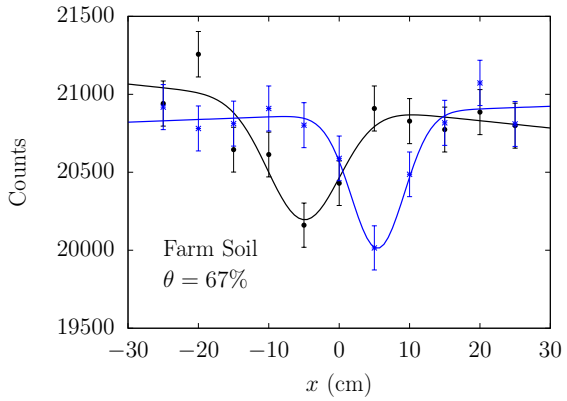

(c) Inversion of the signal obtained for both arrays with $\theta = 67\%$ in farm soil.

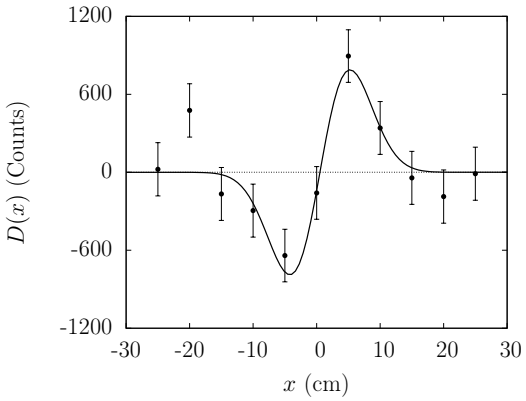

(d) Counts difference function $D(x)$ for $\theta = 67\%$ in farm soil.

Figure 4.7: Simulated signal for different moisture content of $\theta = 67\%$ with the landmine at the surface $d = 0$ cm and the detectors arrays and source at $z = 3$ cm from the surface, for the case of sand and farm soil. And inversion of the signal is detected and could be used for determining the position of the landmine.

If we go beyond the point in which no signal can be defined (critical point) the hydrogen density present in the soil is larger than in the landmine and less neutrons are thermalized in it, than in the surrounding soil. In this case a decrement in the number of detected thermal neutrons is observed in the region of the landmine, this produce an inversion in the detected signal which also can be used to determine the position of the landmine. Figure 4.2 shows the NBT simulated with a moisture content in the soil of 67%.

4.3 Amplitude relation

In figure (4.8) the evolution of the relative amplitude $D_0/D_0(\theta = 0\%)$ as a function of the moisture content θ_m for the landmine (DLM2) placed at $d = 0$ cm, where $D_0(\theta = 0\%)$ is the amplitude obtained for the case of dry sand 4.1. In the case of sand a there is an increasing behavior in the range of $\theta = 0\%-10\%$ which is implies that in this range the amplitude of the signal for the θ specified

is increasing, within a maximum in $\theta = 10\%$ meanwhile in the range of $\theta = 17\% - 34\%$ a decreasing of the obtained signal is present to the region where no signal can be defined $\theta_{critic} = 42\%$ [2], and thermal neutrons backscattered by the landmine (DML2) are almost equal that the thermal neutrons backscattered by the soil with a moisture content. Beyond that point an inversion of the signal is present as showed before, and negatives values for the amplitude are obtained.

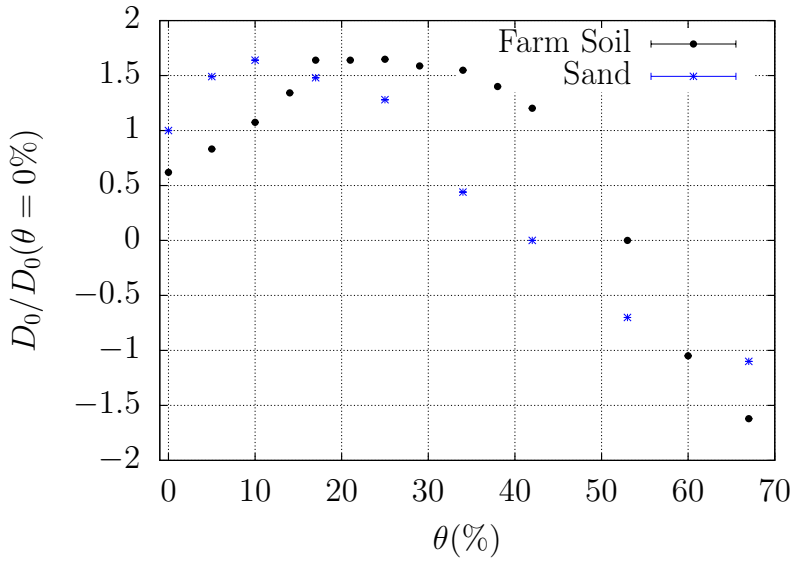

Figure 4.8: Amplitudes relations $D(x)$ distributions relative to the one obtained with dry sand ($\theta = 0\%$) as a function of the moisture content θ. A region in which no signal is obtained is around the critical point $\theta_{critic} = 42\%$ for sand and $\theta_{critic} \backsim 52\%$ for the case of farm soil.

In the case of farm soil a similar behavior is observed, in this case the increasing of the signal goes from $\theta = 0\% - 17\%$ and in the region of $\theta \backsim 25\%$ a maximum is obtained, beyond that point a decreasing of the signal is obtained until the region in which no signal can be defined, and the critical point could be defined for farm soil as $\theta_{critic} \backsim 52\%$. After that point an inversion of the signal is as well obtained.

Chapter 5

Conclusions

- The simulation of NBT in farm soil, shows how the detected signals are strongly dependent of the density of soil which affects directly the mean free path of the neutrons in each kind of soil. In the case of sand the mean free path is smaller than in the case of farm soil which implies more collision between the neutrons and sand, so the neutrons that reach the landmine, they do it with less energy making the process of thermalization easier in the landmine.
- Comparison between the experimental and simulated case shows that the signal generated in both cases are in agreement in the case of sand. Using the same parameters as the experimental case and simulating the time of acquisition for the detector system.
- Simulations with moisture in the soil shows an increment in the detect signal D_0 and background that could be explained as prethermalization process in the wet soil, this process make easier the thermalization process in the landmine. The increment in amplitude in the sand goes up to $\theta = 10\%$ and in farm soil goes up to $\theta = 25\%$ after that point the amplitude of the signal star to decrease until no signal can be obtained (critical point) for sand is about $\theta_c = 42\%$ and for farm soil is $\theta_c = 52\%$. After the critical point in both cases an inversion of the signal is found due that more neutrons thermalize in the wet soil that in the case of the landmine. This inverted signal can be used for determining the location of the mine.

Bibliography

[1] Jacqueline MacDonald and J. R. Lockwood. Alternatives for landmine detection. CA: RAND Corporation, 2003.

[2] Angel Cruz. Neutron backscatering technique for the detection of buried organic objects. Master's thesis, Universidad Nacional de Colombia, 2009.

[3] G. Viesti et. al. The detection of landmines by neutron backscattering: Exploring the limits of the technique. *Applied Radiation and Isotopes*, 64(6):706 – 716, 2006.

[4] F.D. Brooks and M. Drosg. The hydad-d antipersonnel landmine detector. *Applied Radiation and Isotopes*, 63(5–6):565 – 574, 2005.

[5] William Leo. *Techniques for nuclear and particle physics experiments : a how-to approach*. Springer, Berlin New York, 1994.

[6] Glenn Knoll. *Radiation detection and measurement*. John Wiley, Hoboken, N.J, 2010.

[7] C.P. Datema et. al. Experimental results and monte carlo simulations of a landmine localization device using the neutron backscattering method. *Nuclear Instruments and Methods in Physics Research Section A: Accelerators, Spectrometers, Detectors and Associated Equipment*, 488(1–2):441 – 450, 2002.

[8] Wikipedia. Organic matter. http://en.wikipedia.org/wiki/Organic_matter, October 2014.

[9] M. E. Sumner. *Handbook of soil science*. CRC Press, Boca Raton, Fla, 2000.

[10] Jasmina Obhođaš et. al. The soil moisture and its relevance to the landmine detection by neutron backscattering technique. *Nuclear Instruments and Methods in Physics Research Section B: Beam Interactions with Materials and Atoms*, 213(0):445 – 451, 2004.

[11] Cern. Geant4 user documentation. http://geant4.cern.ch/support/userdocuments.shtml, November 2009.

[12] National Nuclear Data Center. Evaluated nuclear data file. http://www.nndc.bnl.gov/exfor/endf00.jsp, November 2014.

[13] INC. LND. Designers and manufacturers of nuclear radiation detectors. http://www.lndinc.com/products/546/, November 2014.